INTERNATIONAL JOURNAL FOR NUMERICAL AND ANALYTICAL METHODS IN GEOMECHANICS
Int. J. Numer. Anal. Meth. Geomech. 2010; **34**:689–709
Published online 17 July 2009 in Wiley InterScience (www.interscience.wiley.com). DOI: 10.1002/nag.825

The fundamental solution of poroelastic plate saturated by fluid and its applications

P. H. Wen[1,*,†] and Y. W. Liu[2]

[1]*School of Engineering and Materials Science, Queen Mary, University of London, London E1 4NS, U.K.*
[2]*College of Mechanics and Aerospace, Hunan University, Changsha 410082, People's Republic of China*

SUMMARY

In this paper, the numerical model of the transverse vibrations of a thin poroelastic plate saturated by a fluid was proposed. Two coupled dynamic equations of equilibrium related to the plate deflection and the equivalent moment were established for an isotropic porous medium with uniform porosity. The fundamental solutions for a porous plate were derived both in the Laplace transform domain and in the time domain. A meshless method was developed and demonstrated in the Laplace transform domain for solving two coupled dynamic equations. Numerical examples demonstrated the accuracy of the method of the fundamental solutions and comparisons were made with analytical solutions. The proposed meshless method was shown to be simple to implement and gave satisfactory results for a poroelastic plate dynamic analysis. Copyright © 2009 John Wiley & Sons, Ltd.

Received 23 January 2009; Revised 16 May 2009; Accepted 25 May 2009

KEY WORDS: poroelastic plate; Laplace transformation; method of fundamental solution; boundary element method; meshless method

1. INTRODUCTION

The vibrations of porous structures are important in the aeronautical industry and in civil engineering, where porous beam and plates are used as sound absorbers. Recently, the use of the poroelastic model has been widely reported in the literature for massive structures in geo-mechanical problems. The deformation in the porous material with coupled fluid movements has been studied quite extensively by a number of researchers, with a wide variety of analytical and numerical methods covering a broad range of both geometric and flow parameters [1]. Modelling of the

*Correspondence to: P. H. Wen, School of Engineering and Materials Science, Queen Mary, University of London, London E1 4NS, U.K.
†E-mail: p.h.wen@qmul.ac.uk

coupled phenomena of fluid flow and deformation of porous materials is a classical problem in geo-mechanics and biomechanics. The theory of deformable porous medium with coupled shear flow movement was investigated by Biot [2, 3] on the consolidation of soil. The linear poroelasticity theory has been applied to many problems in geo-mechanics [3, 4]. This theory has since been extended to the study of biological tissue mechanics [5–8]. Analytical solutions were derived for a 3D fluid-saturated linear poroelastic beams under pure bending and compared with three-dimensional finite element simulations by Wang *et al.* [9]. A numerical procedure was presented by Qiu and Fox [10] for the simulation of 1D compression wave propagation in saturated poroelastic media and the media were modelled as a two-phase system consisting of compressible fluid and solids. Analytical solutions for a shear fluid over a thin deformable porous layer fixed to the wall of two-dimensional channel were found by Barry *et al.* [11] with the assumption that the porosity and permeability are constants. Therefore, the coupled equations are linear and amenable to Fourier analysis. Three situations were considered in their paper, i.e. steady-state deformation, rigid porous layer and deformable porous layer. Wen *et al.* [12] derived the solutions in closed-form for viscous fluid over a deformation porous layer in a cylinder, in Laplace transform space. Numerical simulation for viscous flow in a porous medium has become more and more important over the last two decades. The boundary element method has successfully been developed as a useful numerical technique in solving partial differential equations. Comprehensive discussion and reviews into viscous flow can be found in two recent books by Pozrikidis [13] and Wrobel [14].

For the poroelastic plate problems, a significant result has been given by Theodorakopoulos and Bescos [15]. They extended the classical theory of thin rectangular plates to porous materials including Biot's stress–strain relations in porous media [16]. Leclaire *et al.* [17] have proposed two equations of equilibrium, which are valid in applications where the plate is thinner than any acoustic wavelength. A variational method for solving the rectangular plate equations was developed by Leclaire *et al.* [18] for different porous materials with four edges clamped. Based on the theory of porous media, a dynamic bending model of incompressible saturated rectangular poroelastic plate simply supported with in-plane diffusion was analysed by He and Yang [19] and analytical solutions using the Fourier series method were presented.

Meshless methods, such as the method of fundamental solution (MFS) and method of particular solution (MPS) [20–22], meshfree Galerkin method [23] and meshless Petrov–Galerkin method [24], have attracted great attention for numerically solving time-dependent problems. Various meshless methods have been developed and successfully employed to solve challenging problems in different areas of science and engineering. Cheng and Cabral [20] presented a different approach for solving ill-posed boundary value problems by introducing a numerical technique based on the radial basis function collocation method for the solution of well-posed boundary value problems. The MFS and MPS have been shown to be accurate for solving homogeneous equation if the fundamental solution of the given differential operator by Chen *et al.* [21]. However, the fundamental solution of a given differential equation is not always available and the ill conditioning of the MFS and the location of source points are also issues to be resolved. Cheng and Cabral [20] solved the interior and exterior Laplace problems with a circular boundary and prove the mathematical equivalence between the Trefftz method and the MFS. In this paper, the MFSs have been derived to solve the poroelastic plates first time subjected to a dynamic load using Laplace transform method. By considering the boundary conditions, it was possible to determine all the coefficients of the fundamental solutions. Several numerical examples are given to demonstrate the accuracy of the propose approach compared with analytical solutions.

DOI: 10.1002/nag

2. FUNDAMENTAL EQUATIONS OF POROELASTIC PLATE

For a binary incompressible elastic non-capillary porous media, the fundamental equations can be expressed, see Boer [25], as

$$(\lambda_S+\mu_S)\boldsymbol{\Delta}\mathbf{u}^{\mathrm{S}}+\mu_S\mathrm{div}\,\mathbf{u}^{\mathrm{S}}-n_S\nabla p-S_L[\dot{\mathbf{u}}^{\mathrm{S}}-\dot{\mathbf{u}}^{\mathrm{L}}]+\rho_S\mathbf{b}=\rho_S\ddot{\mathbf{u}}^{\mathrm{S}} \tag{1a}$$

$$-n_L\nabla p-S_L[\dot{\mathbf{u}}^{\mathrm{L}}-\dot{\mathbf{u}}^{\mathrm{S}}]^{+}\rho_L\mathbf{b}=\rho_L\ddot{\mathbf{u}}^{\mathrm{L}} \tag{1b}$$

$$\mathrm{div}\,(n_S\dot{\mathbf{u}}^{\mathrm{S}}+n_L\dot{\mathbf{u}}^{\mathrm{L}})=\mathbf{0} \tag{1c}$$

where λ_S and μ_S are the Lamé constants of solid skeleton; n_S, n_L are volume fractions for solid and fluid, respectively; S_L is scalar response parameter ($=n_L^2\mu/k$), here μ is fluid viscosity and k Darcy's coefficient of permeability; $\mathbf{u}^{\mathrm{S}}$ and $\mathbf{u}^{\mathrm{L}}$ are displacement vectors; ρ_S and ρ_L are densities of solid and fluid, p is the fluid pressure in the pores; $\dot{F}=\partial F/\partial t$. Considering the relationship $n_S+n_L=1$ and introducing $\mathbf{w}^{\mathrm{L}}=\dot{\mathbf{u}}^{\mathrm{L}}-\dot{\mathbf{u}}^{\mathrm{S}}$, which is the relative velocity of fluid to the solid, Equation (1) can be arranged as [26]

$$\mathrm{div}\,\boldsymbol{\sigma}^{\mathrm{S}}-\nabla p+\rho[\mathbf{b}-\ddot{\mathbf{u}}^{\mathrm{S}}]^{-}\rho_L\dot{\mathbf{w}}^{\mathrm{L}}=\mathbf{0} \tag{2a}$$

$$-n_L\nabla p+\rho_L[\mathbf{b}-\ddot{\mathbf{u}}^{\mathrm{S}}-\dot{\mathbf{w}}^{\mathrm{L}}]^{-}S_L\mathbf{w}^{\mathrm{L}}=\mathbf{0} \tag{2b}$$

$$\mathrm{div}(\dot{\mathbf{u}}^{\mathrm{S}}+n_L\mathbf{w}^{\mathrm{L}})=\mathbf{0} \tag{2c}$$

where $\boldsymbol{\sigma}^{\mathrm{S}}$ is the tensor of stress in the solid and $\rho=\rho_S+\rho_L$ is the density of the mixture body. In general, the boundary conditions can be given for the media of solid as

$$\begin{aligned}\mathbf{u}^{\mathrm{S}}&=\mathbf{u}_0^{\mathrm{S}},\quad \mathbf{x}\in\Gamma_u\\ \mathbf{t}^{\mathrm{S}}&=\mathbf{t}_0^{\mathrm{S}},\quad \mathbf{x}\in\Gamma_t\end{aligned} \tag{3}$$

where Γ_u and Γ_t are displacement and traction boundaries, $\mathbf{t}^{\mathrm{S}}=\mathbf{n}\cdot(\boldsymbol{\sigma}^{\mathrm{S}}-p\mathbf{I})$, in which $\mathbf{I}$ is the identity matrix. For the fluid, the boundary conditions are given by

$$\begin{aligned}p&=p_0,\quad \mathbf{x}\in\Gamma_p\\ U&=U_0,\quad \mathbf{x}\in\Gamma_U\end{aligned} \tag{4}$$

in which Γ_p, Γ_U are pressure and velocity boundaries, respectively, $U=\mathbf{n}\cdot(n_L\mathbf{w}^{\mathrm{L}})$. Assume that the solid and fluid are initially at rest, i.e. the initial condition of the mixture body is given by

$$\mathbf{u}^{\mathrm{S}}=\mathbf{0},\quad \dot{\mathbf{u}}^{\mathrm{S}}=\mathbf{0},\quad \mathbf{w}^{\mathrm{L}}=\mathbf{0},\quad t=0,\quad \mathbf{x}\in V \tag{5}$$

Consider a poroelastic plate of thickness h and assume that the body force $\mathbf{b}=\mathbf{0}$, densities ρ_S, ρ_L and the scalar parameter S_L are assumed to be constants. In addition, there are no shear forces acting on the surfaces of plate, i.e. $\sigma_{13}^{\mathrm{S}}=\sigma_{23}^{\mathrm{S}}=0$. Let $\mathbf{u}^{\mathrm{S}}=(u_1^{\mathrm{S}},u_2^{\mathrm{S}},u_3^{\mathrm{S}})$, $\mathbf{w}^{\mathrm{L}}=(w_1^{\mathrm{L}},w_2^{\mathrm{L}},w_3^{\mathrm{L}})$ in thin plate theory, the in-plane displacements can be written as

$$u_1^{\mathrm{S}}=-x_3\frac{\partial w}{\partial x_1},\quad u_2^{\mathrm{S}}=-x_3\frac{\partial w}{\partial x_2},\quad u_3^{\mathrm{S}}=w \tag{6}$$

DOI: 10.1002/nag

Furthermore, the relative velocity in the plate is assumed $w_3^{\mathrm{L}}=0$. Multiplying with x_3 and integrating along the thickness, (2a), (2b) and (2c) give

$$M^{\mathrm{S}}_{\alpha\beta,\beta}-M_{p,\alpha}-Q^{\mathrm{S}}_{\alpha}+\frac{\rho h^3}{12}\ddot{w}_{,\alpha}-\rho_L\dot{\bar{w}}^{\mathrm{L}}_{\alpha}=0,\quad \alpha=1,2 \tag{7a}$$

$$n_L M_{p,\alpha}+\rho_L\left(\dot{\bar{w}}^{\mathrm{L}}_{\alpha}-\frac{h^3}{12}\dot{w}_{,\alpha}\right)+S_L\bar{w}^{\mathrm{L}}_{\alpha}=0,\quad \alpha=1,2 \tag{7b}$$

$$-\frac{h^3}{12}\nabla^2\dot{w}+n_L\bar{w}^{\mathrm{L}}_{\beta,\beta}=0 \tag{7c}$$

where the stress moment resultants are defined as

$$M_{\alpha\beta}=\int_{-h/2}^{h/2}\sigma^{\mathrm{S}}_{\alpha\beta}x_3\,\mathrm{d}x_3 \tag{8}$$

In the same way, integrating with respect to x_3 results gives

$$Q^{\mathrm{S}}_{\beta,\beta}+q-\rho h\ddot{w}=0 \tag{9}$$

where $q=(\sigma^{\mathrm{S}}_{33}-p)^{x_3=h/2}_{x_3=-h/2}$, which represents the applied load on the top and bottom surfaces of plate, and resultants of shear force and the average relative velocity are defined by

$$Q^{\mathrm{S}}_{\alpha}=\int_{-h/2}^{h/2}\sigma^{\mathrm{S}}_{\alpha 3}\,\mathrm{d}x_3,\quad \bar{w}_{L\alpha}=\int_{-h/2}^{h/2}w_{L\alpha}\,\mathrm{d}x_3 \tag{10}$$

By using the following constitutive relations for the thin plate bending:

$$M^{\mathrm{S}}_{11}=-D\left(\frac{\partial^2 w}{\partial x_1^2}+\nu_S\frac{\partial^2 w}{\partial x_2^2}\right) \tag{11a}$$

$$M^{\mathrm{S}}_{22}=-D\left(\frac{\partial^2 w}{\partial x_2^2}+\nu_S\frac{\partial^2 w}{\partial x_1^2}\right) \tag{11b}$$

$$M^{\mathrm{S}}_{12}=-(1-\nu_S)D\frac{\partial^2 w}{\partial x_1\partial x_2} \tag{11c}$$

and

$$Q^{\mathrm{S}}_{1}=-D\frac{\partial}{\partial x_1}(\nabla^2 w) \tag{12a}$$

$$Q^{\mathrm{S}}_{2}=-D\frac{\partial}{\partial x_2}(\nabla^2 w) \tag{12b}$$

where $D=E_S h^2/12(1-\nu_S^2)$ is the flexural rigidity of the poroelastic plate, we obtain one of the fundamental equations, from (7a), as

$$D\nabla^2\nabla^2 w+\nabla^2 M_p-\frac{\rho h^3}{12}\nabla^2\ddot{w}+\rho_L\dot{\bar{w}}^{\mathrm{L}}_{\beta,\beta}+\rho h\ddot{w}=q \tag{13}$$

DOI: 10.1002/nag

Considering the relationship in Equation (7c), Equation (13) becomes

$$D\nabla^2\nabla^2 w+\nabla^2 M_p-\frac{h^3\rho}{12}\left(1-\frac{\rho_L}{n_L\rho}\right)\nabla^2\ddot{w}+\rho h\ddot{w}=q \tag{14}$$

and then (7b) can be simplified as

$$\frac{h^3 S_L}{12n_L^2}\nabla^2\dot{w}-\frac{h^3(1-n_L)\rho_L}{12n_L^2}\nabla^2\ddot{w}+\nabla^2 M_p=0 \tag{15}$$

Therefore, the deflection w and equivalent moment M_p can be solved from (14) and (15). The relative velocities $\bar{w}_\alpha^{\mathrm{L}}(\alpha=1,2)$ can be solved from (7b). By ignoring the effect of in-plane inertial terms in poroelastic plate, (14), (15) and (7b) can be simplified further as [6]

$$D\nabla^2\nabla^2 w+\nabla^2 M_p+\rho h\ddot{w}=q \tag{16a}$$

$$\frac{h^3 S_L}{12n_L^2}\nabla^2\dot{w}+\nabla^2 M_p=0 \tag{16b}$$

$$n_L M_{p,\alpha}+S_L\bar{w}_{L\alpha}=0 \tag{16c}$$

Above equations are the fundamental equations for poroelastic plates with four variables w, M_p, $\bar{w}_1^{\mathrm{L}}$ and $\bar{w}_2^{\mathrm{L}}$. Following the same treatment to the Biot's model [16], the fundamental equations can be derived as [26]

$$D\nabla^2\nabla^2 w+\frac{R+Q}{R}n_L\nabla^2 M_p+\rho h\ddot{w}=q \tag{17a}$$

$$\frac{h^3 S_L(Q+R)}{12n_L^2 R}\nabla^2\dot{w}-\frac{S_L}{R}\dot{M}_p+\nabla^2 M_p=0 \tag{17b}$$

where R and Q are elastic coefficients in Biot's model [3, 16]. Introducing non-dimension notations as follows:

$$\begin{aligned} x_i^* &= x_i/a, \quad w^*=w/h, \quad t^*=t/\beta, \quad S_L^*=S_L h^3 a^2/D\beta \\ q^* &= qa^4/Dh, \quad \beta=a^2\sqrt{\rho h/D} \\ M_{\alpha\beta}^* &= M_{\alpha\beta}^{\mathrm{S}}\,a^2/Dh, \quad K=S_L^*/12n_L^2 \\ K &= S_L^*/12n_L^2, \quad M_p^*=a^2 M_p/Dh \end{aligned} \tag{18}$$

The fundamental equations (14) and (15) can be written as

$$\nabla^{*2}\nabla^{*2}w^*+\nabla^{*2}M_p^*+K_2\nabla^{*2}\ddot{w}^*+\ddot{w}^*=q^* \tag{19a}$$

$$K\nabla^2\dot{w}^*-K_1\nabla^{*2}\ddot{w}^*+\nabla^2 M_p^*=0 \tag{19b}$$

where $\nabla^{*2}=\partial^2/\partial x_1^{*2}+\partial^2/\partial x_2^{*2}$ and non-dimensional parameters

$$K_1=\frac{1-n_L}{12n_L^2}\left(\frac{\rho_L}{\rho}\right)\left(\frac{h}{a}\right)^2, \quad K_2=\frac{1}{12}\left(\frac{h}{a}\right)^3\left[1-\frac{1}{n_L}\left(\frac{\rho_L}{\rho}\right)\right] \tag{20}$$

DOI: 10.1002/nag

By ignoring the effect of inertial terms in plate, i.e. $K_1=K_2=0$ in (19), we obtain

$$\nabla^{*2}\nabla^{*2}w^*+\nabla^{*2}M_p^*+\ddot{w}^*=q^* \tag{21a}$$

$$K\nabla^{*2}\dot{w}^*+\nabla^{*2}M_p^*=0 \tag{21b}$$

Simplified dimensionless fundamental equations of Biot's model in (17a) and (17b) can be written as

$$\nabla^{*2}\nabla^{*2}w^*+(1-\varepsilon_1)\nabla^{*2}M_p^*+\ddot{w}^*=q^* \tag{22a}$$

$$K(1-\varepsilon_1)\nabla^{*2}\dot{w}^*-\varepsilon_2\dot{M}_p^*+\nabla^{*2}M_p^*=0 \tag{22b}$$

where ε_1 and ε_2 are two non-dimensional parameters in Biot's model [3, 16, 26] and can be obtained from (19a) and (19b) directly as

$$\varepsilon_1=1-\frac{Q+R}{R}n_L, \quad \varepsilon_2=\frac{DS_L^*}{Rh^3} \tag{22c}$$

3. FUNDAMENTAL SOLUTIONS FOR POROELASTIC PLATES

For convenience, the superscripts '$*$' will be omitted in the following analysis. Applying the Laplace transform to the fundamental equations with initial condition of the mixture body in (22a) and (22b) yields

$$\nabla^2\nabla^2\tilde{w}+(1-\varepsilon_1)\nabla^2\tilde{M}_p+s^2\tilde{w}=\tilde{q} \tag{23a}$$

$$K(1-\varepsilon_1)\nabla^2\tilde{w}-\varepsilon_2 s\tilde{M}_p+\nabla^2\tilde{M}_p=0 \tag{23b}$$

where the transformation in the Laplace domain of a function $f(\mathbf{x},t)$ is defined as

$$L[f(\mathbf{x},t)]=\tilde{f}(\mathbf{x},s)=\int_0^\infty f(\mathbf{x},t)\mathrm{e}^{-st}\,\mathrm{d}t \tag{24}$$

in which s is the parameter of the Laplace transformation. If $\tilde{q}=0$, eliminating $\tilde{M}_p$ from (23b) and (23a) gives a governing equation of $\tilde{w}$

$$\nabla^2\nabla^2\nabla^2\tilde{w}+[K(1-\varepsilon_1)^2+\varepsilon_2]^s\nabla^2\nabla^2\tilde{w}+s^2\nabla^2\tilde{w}-s^3\varepsilon_2\tilde{w}=0 \tag{25a}$$

The equivalent moment can be determined in the transformed domain as

$$\tilde{M}_p=\frac{1}{\varepsilon_2(1-\varepsilon_1)s}[K(1-\varepsilon_1)^2s\nabla^2\tilde{w}-s^2\tilde{w}-\nabla^2\nabla^2\tilde{w}] \tag{25b}$$

The fundamental solutions for a poroelastic plate can be written, from (25a), as

$$\tilde{w}=\sum_{k=1}^{3}A_kK_0(\sqrt{s\xi_k}r)+\sum_{k=1}^{3}B_kK_0(\sqrt{s\xi_k}r) \tag{26}$$

where non-dimensional parameters ξ_k are three roots in the following equation as

$$\xi^3+[K(1-\varepsilon_1)^2+\varepsilon_2]^{\xi 2}+\xi-\varepsilon_2=0 \tag{27}$$

DOI: 10.1002/nag

and A_k and B_k are unknowns coefficients that are to be determined by considering the boundary conditions. Considering the fundamental solutions in an infinite plate, we should have $B_k=0$. The fundamental solutions of moment can be expressed, from (11), as

$$\tilde{M}_{11}=-\sum_{k=1}^{3}\frac{A_k\sqrt{s\xi_k}}{r^3}[(1-\nu^{\mathrm{S}})(x_1^2-x_2^2)K_1(\sqrt{s\xi_k}r)+(x_1^2+\nu^S x_2^2)\sqrt{s\xi_k}rK_0(\sqrt{s\xi_k}r)]$$

$$=\sum_{k=1}^{3}f_{11k}(x_1,x_2)A_k \tag{28a}$$

$$\tilde{M}_{22}=-\sum_{k=1}^{3}\frac{A_k\sqrt{s\xi_k}}{r^3}[(1-\nu^{\mathrm{S}})(x_2^2-x_1^2)K_1(\sqrt{s\xi_k}r)+(x_2^2+\nu^S x_1^2)\sqrt{s\xi_k}rK_0(\sqrt{s\xi_k}r)]$$

$$=\sum_{k=1}^{3}f_{22k}(x_1,x_2)A_k \tag{28b}$$

$$\tilde{M}_{12}=-(1-\nu^{\mathrm{S}})\sum_{k=1}^{3}\frac{x_1x_2A_k\sqrt{s\xi_k}}{r^3}[2K_1(\sqrt{s\xi_k}r)+\sqrt{s\xi_k}rK_0(\sqrt{s\xi_k}r)]$$

$$=\sum_{k=1}^{3}f_{12k}(x_1,x_2)A_k \tag{28c}$$

shear forces from (12)

$$\tilde{Q}_1=-\sum_{k=1}^{3}\frac{x_1A_k\sqrt{(s\xi_k)^3}}{r}K_1(\sqrt{s\xi_k}r)=\sum_{k=1}^{3}g_{1k}(x_1,x_2)A_k \tag{29a}$$

$$\tilde{Q}_2=-\sum_{k=1}^{3}\frac{x_2A_k\sqrt{(s\xi_k)^3}}{r}K_1(\sqrt{s\xi_k}r)=\sum_{k=1}^{3}g_{2k}(x_1,x_2)A_k \tag{29b}$$

and equivalent moment by the pressure in porous of plate from (25b)

$$\tilde{M}_p=\frac{s}{\varepsilon_2(1-\varepsilon_1)}\sum_{k=1}^{3}[K(1-\varepsilon_1)^2\xi_k-1-\xi_k^2]A_kK_0(\sqrt{s\xi_k}r)=\sum_{k=1}^{3}m_k(x_1,x_2)A_k \tag{30}$$

From above fundamental solutions, the fundamental solutions of a concentrated shear force in a poroelastic plate can be derived easily. Considering a concentrated force at origin

$$q(t)=\delta(\mathbf{x})\delta(t) \tag{31}$$

and transformed concentrated force in the Laplace domain is $\tilde{q}(s)=\delta(\mathbf{x})$. The conditions to determine three unknown coefficients should be

$$\left.\frac{\partial\tilde{w}}{\partial r}\right|_{r=0}=0,\quad 2\pi r\tilde{Q}_r|_{r=0}=1,\quad \left.\frac{\partial\tilde{M}_p}{\partial r}\right|_{r=0}=0 \tag{32}$$

DOI: 10.1002/nag

Substituting (26), (29) and (30) into (32) results

$$A_1+A_2+A_3=0 \tag{33a}$$

$$2\pi(\xi_1^2A_1+\xi_2^2A_2+\xi_3^2A_3)s=1 \tag{33b}$$

$$[K(1-\varepsilon_1)^2\xi_1-1-\xi_1^2]A_1+[K(1-\varepsilon_1)^2\xi_2-1-\xi_2^2]A_2+[K(1-\varepsilon_1)^2\xi_3-1-\xi_3^2]A_3=1 \tag{33c}$$

Solving the above equations, we obtain

$$\tilde{w}(r)=\frac{1}{2\pi(\alpha_1\xi_1^2+\alpha_2\xi_2^2+\alpha_3\xi_3^2)}\frac{1}{s}\sum_{k=1}^{3}\alpha_k K_0(\sqrt{s\xi_k}r) \tag{34}$$

where

$$\begin{aligned}\alpha_1&=\frac{[K(1-\varepsilon_1)^2-\xi_2]\xi_2-[K(1-\varepsilon_1)^2-\xi_3]\xi_3}{[K(1-\varepsilon_1)^2-\xi_1]\xi_1-[K(1-\varepsilon_1)^2-\xi_2]\xi_2}\\ \alpha_2&=\frac{[K(1-\varepsilon_1)^2-\xi_1]\xi_1-[K(1-\varepsilon_1)^2-\xi_3]\xi_3}{[K(1-\varepsilon_1)^2-\xi_2]\xi_2-[K(1-\varepsilon_1)^2-\xi_1]\xi_1}\\ \alpha_3&=1\end{aligned} \tag{35}$$

Then, by substituting coefficients into (28), (29) and (30), the fundamental solutions of moment, shear force and equivalent moment are obtained in the Laplace transform domain. In addition, the fundamental solution of deformation of poroelastic plate $w(r,t)$ in the time domain, can be arranged [27] as

$$w(r,t)=\frac{1}{4\pi(\alpha_1\xi_1^2+\alpha_2\xi_2^2+\alpha_3\xi_3^2)}\sum_{k=1}^{3}\alpha_k E_1\left(\frac{\xi_k r^2}{4t}\right) \tag{36}$$

where $E_1(z)$ is the exponential integral and defined as

$$E_1(z)=\int_z^\infty \frac{\mathrm{e}^{-u}}{u}\,\mathrm{d}u \tag{37}$$

This function can be expressed in series form as

$$E_1(z)=-\gamma-\ln z-\sum_{n=1}^{\infty}\frac{(-1)^n z^n}{nn!} \tag{38}$$

where $\gamma=0.5772156649$ is Euler's constant. The fundamental solutions of moment and shear force can be obtained in the time domain as follows:

$$M_{11}=-\frac{1}{2\pi r^4(\alpha_1\xi_1^2+\alpha_2\xi_2^2+\alpha_3\xi_3^2)}\sum_{k=1}^{3}\left[(1-v^{\mathrm{S}})(x_1^2-x_2^2)+\frac{\xi_k}{4t}r^2(x_1^2+v^S x_2^2)\right]\alpha_k\mathrm{e}^{-\xi_k r^2/4t} \tag{39a}$$

$$M_{22}=-\frac{1}{2\pi r^4(\alpha_1\xi_1^2+\alpha_2\xi_2^2+\alpha_3\xi_3^2)}\sum_{k=1}^{3}\left[(1-v^{\mathrm{S}})(x_2^2-x_1^2)+\frac{\xi_k}{4t}r^2(x_2^2+v^S x_1^2)\right]\alpha_k\mathrm{e}^{-\xi_k r^2/4t} \tag{39b}$$

$$M_{12}=\frac{(1-v^{\mathrm{S}})x_1x_2}{2\pi r^4(\alpha_1\xi_1^2+\alpha_2\xi_2^2+\alpha_3\xi_3^2)}\sum_{k=1}^{3}\left(2+\frac{\xi_k r^2}{4t}\right)\alpha_k\mathrm{e}^{-\xi_k r^2/4t} \tag{39c}$$

DOI: 10.1002/nag

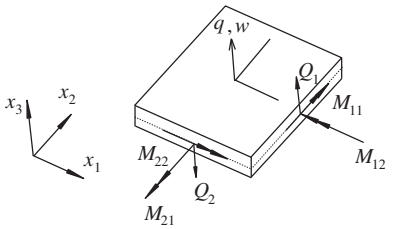

Figure 1. Sign convention of displacement and internal forces.

$$Q_1 = \frac{x_1}{8\pi r^4(\alpha_1\xi_1^2+\alpha_2\xi_2^2+\alpha_3\xi_3^2)t^2}\sum_{k=1}^{3}\alpha_k\xi_k^2 e^{-\xi_k r^2/4t} \tag{40a}$$

$$Q_2 = \frac{x_2}{8\pi r^4(\alpha_1\xi_1^2+\alpha_2\xi_2^2+\alpha_3\xi_3^2)t^2}\sum_{k=1}^{3}\alpha_k\xi_k^2 e^{-\xi_k r^2/4t} \tag{40b}$$

and the equivalent moment

$$M_p(t) = \frac{1}{4\pi(\alpha_1\xi_1^2+\alpha_2\xi_2^2+\alpha_3\xi_3^2)t^2}\sum_{k=1}^{3}[K(1-\varepsilon_1)^2\xi_k - 1 - \xi_k^2]\left(\frac{\xi_k r^2}{4t}-1\right)\alpha_k\xi_k^2 e^{-\xi_k r^2/4t} \tag{41}$$

The above fundamental solution (concentrated force) can be used to derive the boundary integral formulations for the poroelastic plate problem (Figure 1).

4. METHOD OF FUNDAMENTAL SOLUTIONS IN LAPLACE DOMAIN

In the MFS, we allocate source points outside the physical domain in order to avoid the singularities in the fundamental solutions. By using the principle of superposition for linear elasticity, Wen [28, 29] demonstrated the MFS for Kirchhoff plate resting on an elastic foundation subjected to static loads. In the case of a poroelastic plate with a curvilinear boundary, a series points **P** (collocation points) on the edge of boundary are considered as shown in Figure 2. As the superposition principle is still valid in the transformed domain, the approximate solutions of the deflection, moments, shear forces and equivalent moment in the Laplace domain on the collocation point can be presented as [30]

$$\tilde{w}(\mathbf{P}) = \tilde{w}^0(\mathbf{P}) + \sum_{n=1}^{N}\sum_{k=1}^{3} K_0(\sqrt{s\xi_k}r)A_k^n(\mathbf{Q}) \tag{42a}$$

$$\tilde{M}_n(\mathbf{P}) = \tilde{M}_n^0(\mathbf{P}) + \sum_{n=1}^{N}\sum_{k=1}^{3}(f_{11k}^n n_1^2 + f_{22k}^n n_2^2 - 2f_{11k}^n n_1 n_2)A_k^n(\mathbf{Q}) \tag{42b}$$

$$\tilde{M}_t(\mathbf{P}) = \tilde{M}_t^0(\mathbf{P}) + \sum_{n=1}^{N}\sum_{k=1}^{3}(f_{12k}^n[n_1^2-n_2^2] - [f_{11k}^n - f_{22k}^n]n_1 n_2)A_k^n(\mathbf{Q}) \tag{42c}$$

DOI: 10.1002/nag

$$\tilde{Q}_n(\mathbf{P}) = \tilde{Q}_n^0(\mathbf{P}) + \sum_{n=1}^{N}\sum_{k=1}^{3}(g_{\beta k}^n n_\beta) A_k^n(\mathbf{Q}) \tag{42d}$$

$$\tilde{M}_p(\mathbf{P}) = \tilde{M}_p^0(\mathbf{P}) + \sum_{n=1}^{N}\sum_{k=1}^{3} m_k^n A_k^n(\mathbf{Q}) \tag{42e}$$

where $r = r(\mathbf{P}, \mathbf{Q})$; $\tilde{w}^0(\mathbf{P})$, $\tilde{M}_n^0(\mathbf{P})$, $\tilde{M}_t^0(\mathbf{P})$ and $\tilde{M}_p^0(\mathbf{P})$ present the particular solutions in governing equations (22a) and (22b); $\mathbf{P}$ and $\mathbf{Q}$ denote the collocation and source points (fundamental solution) as shown in Figure 2 and n_β represents the component of the outward normal vector to the boundary of the plate. $A_k^n(\mathbf{Q})(k = 1, 2, 3; n = 1, 2, \ldots, N)$ are unknown coefficients of the fundamental solution on the source point n. In general case, the number of collocation point on the real boundary N_c is different from the number of source point outside of domain N_s. The least-square method needs to be utilized to determine all unknown densities if $N_c > N_s$. In this paper, the case $N_c = N_s$ is considered only.

In general, the applied load on the plate surface is a function of coordinate. However, if uniform and linear distributed loads are considered in the domain, i.e. [30]

$$q(\mathbf{P}, t) = q_0(t) + q_1(t)x_1 + q_2(t)x_2 \tag{43}$$

where $q_0(t)$, $q_1(t)$ and $q_2(t)$ are time-dependent functions only, we are able to obtain the particular solutions in the Laplace domain analytically as

$$\tilde{q}(\mathbf{P}) = \tilde{q}_0(s) + \tilde{q}_1(s)x_1 + \tilde{q}_2(s)x_2 \tag{44}$$

where particular solutions of displacement can be obtained from the governing equation (4) and are given by

$$\tilde{w}^0 = \frac{1}{s^2}[\tilde{q}_0(s) + \tilde{q}_1(s)x_1 + \tilde{q}_2(s)x_2] \tag{45}$$

and the particular solutions for the moment and the shear forces are

$$\tilde{M}_n^0 = \tilde{M}_t^0 = \tilde{Q}_n^0 = \tilde{M}_p^0 = 0 \tag{46}$$

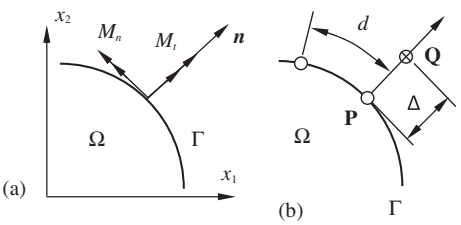

Figure 2. Boundary collocations and source points: (a) convention of traction on the boundary and (b) collocation ($\mathbf{P}$) and source ($\mathbf{Q}$) points.

DOI: 10.1002/nag

Considering a simply supported plate, the displacement and traction boundary conditions of the plate can be written as:

$$\sum_{n=1}^{N}\sum_{k=1}^{3} K_0(\sqrt{s\xi_k}r)A_k^n(\mathbf{Q}) = \tilde{w}_0(\mathbf{P}) - \tilde{w}^0(\mathbf{P}) \tag{47a}$$

$$\sum_{n=1}^{N}\sum_{k=1}^{3} (f_{11k}^n n_1^2 + f_{22k}^n n_2^2 - 2f_{11k}^n n_1 n_2)A_k^n(\mathbf{Q}) = \tilde{M}_{n0}\mathbf{P}) - \tilde{M}_n^0(\mathbf{P}) \tag{47b}$$

$$\sum_{n=1}^{N}\sum_{k=1}^{3} m_k^n A_k^n(\mathbf{Q}) = \tilde{M}_{p0}(\mathbf{P}) - \tilde{M}_p^0(\mathbf{P}) \tag{47c}$$

where $\tilde{w}_0$, $\tilde{M}_{n0}$ and $\tilde{M}_{p0}$ are specified displacement and traction boundary values in the Laplace domain, respectively. Thus, all unknown coefficients in fundamental solutions can be obtained by solving the linear system in (47) in Laplace domain for each parameter s_l, $l=0, 1, 2 \ldots L$. Although the MGS with linear algebraic equations is ill conditioned, the stable and convergent solutions can be obtained by selecting a proper gap between the collocation and source points.

A total number of samples $(L+1)$ in the transformation space s_l are selected. Then the physical variables in time domain can be determined by the inversion technique of the Laplace transform. Here, the method proposed by Durbin [31] is adopted. Demonstration of Durbin's inverse method was made by Wen *et al.* [32] for the elasticity wave propagations for three-dimensional problems. The formula of inversion is written as

$$f(t) = \frac{2\mathrm{e}^{\eta t}}{T}\left[-\frac{1}{2}\tilde{f}(\eta/T) + \sum_{l=0}^{L}\mathrm{Re}\{\tilde{f}(s_l)\mathrm{e}^{2l\pi\mathrm{i}/T}\}\right] \tag{48}$$

in which $\tilde{f}(s_l)$ is the transformed variable in the transformed domain and the parameter $s_l = (\eta + 2l\pi\mathrm{i})/T\,(\mathrm{i}=\sqrt{-1})$. The selection of two free parameters η and T affects the accuracy of inversion slightly. In the following examples, $L=200$, $\eta=5$.

5. EXAMPLES AND DISCUSSIONS

5.1. A square poroelastic plate

Consider a simply supported square plate of length a and thickness h subjected to a uniform dynamic load $q(t)=q_0H(t)$. The aim of this example is to demonstrate the accuracy and the stability of the MGS for selections of the distribution of source points. In this example, Poisson's ratio $v_S=0.3$. Non-dimensional parameters are chosen to be $K=0.5$, $\varepsilon_1=0.05$ and $\varepsilon_2=0.01$ in Biot's model. The relative mean errors (ME) of the deflection and moments at the centre of plate are defined as follows:

$$\mathrm{ME}w = \frac{1}{|w_{\max}|N_t}\sum_{i=1}^{N_t}|w(x_1,x_2,t_i) - \hat{w}(x_1,x_2,t_i)| \tag{49a}$$

$$\mathrm{ME}M_{11} = \frac{1}{|M_{11\max}|N_t}\sum_{i=1}^{N_t}|M_{11}(x_1,x_2,t_i) - \hat{M}_{11}(x_1,x_2,t_i)| \tag{49b}$$

$$\mathrm{ME}M_p = \frac{1}{|M_{p\max}|N_t}\sum_{i=1}^{N_t}|M_p(x_1,x_2,t_i) - \hat{M}_p(x_1,x_2,t_i)| \tag{49c}$$

DOI: 10.1002/nag

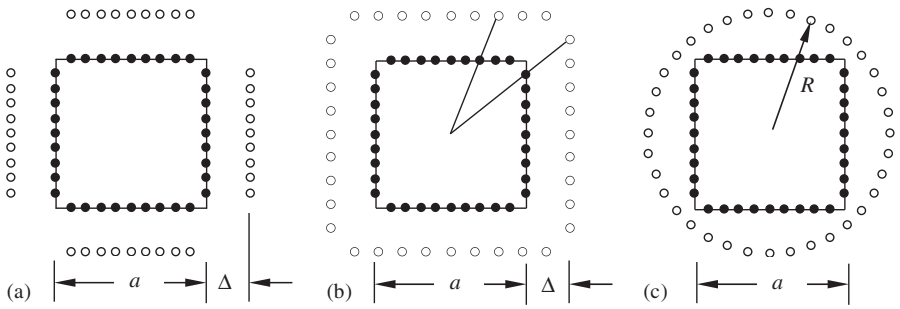

Figure 3. The types of source point distribution: (a) normal distribution; (b) radial distribution; and (c) circular distribution.

where N_t is the number of testing of time, here it is selected as 141 and $t_i = 0.01i$; $\hat{w}$, $\hat{M}_{11}$ and $\hat{M}_p$ represent the analytical solutions, which are derived in the Appendix, $|w_{\max}|$, $|M_{11\max}|$ and $|M_{p\max}|$ are maximum values for the deflection and moments in the region $0 \leqslant t \leqslant 1.4$, in this case, $|w_{\max}| = 0.0059 |M_{11\max}| = 0.0714$ and $|M_{p\max}| = 0.0294$ from analytical solutions in the Appendix. Three types of distribution of source points are proposed as shown in Figure 3, where Δ presents the gap between the collocation and source points. For the first type, the source point is located in the normal direction to collocation point (normal distribution). The second type is that the configuration of the connections of the source points remains the same shape of the boundary (radial distribution). The third type is that the source points are located on a circle (circular distribution). When the total number of collocation points $N = 19 \times 4 = 76$ and $T = 20$, the relative mean errors at the middle of plate are shown in Figures 4(a), (b) and (c), respectively. Apparently for the first type of source point, the relative mean errors are less than 1% for the deflection $w(t)$, moments $M_{11}(t)$ and $M_p(t)$ if $0.2 \leqslant \Delta \leqslant 1$. For the second type and third type, the convergent region are $0.1 \leqslant \Delta \leqslant 0.6$ and $0.3 \leqslant \Delta \leqslant 0.9$, respectively. Obviously, the degree of accuracy for these three types is almost the same. However, the convergence region of selection Δ for the first type is wider than other two types. In addition, Figure 5 shows the accuracy when $N = 9 \times 4 = 36$ for the first type of source point. The convergence region becomes $0.4 \leqslant \Delta \leqslant 2$. Therefore, we could introduce a new non-dimensional parameter Δ/d to define the convergence region, where d is the distance between two collocation points on the boundary. In the example above, the convergent region for the first type is $4 \leqslant \Delta/d \leqslant 20$.

To demonstrate the application of the proposed method to the practical problems in geomechanical engineering, the Boise sandstone [26, 17] is considered and the properties are displayed in Table I. The conversion to and from the present set follows the formulas below:

$$R = \frac{n_L^2 (K_u - K_0)}{\alpha^2}, \quad Q = \frac{n_L (\alpha - n_L)(K_u - K_0)}{\alpha^2}$$

where K_0 and K_u are drained and undrained bulk modulus of elasticity, respectively. Therefore, all parameters are evaluated as in this modelling: $D = 1.029 \times 10^5$ Nm, $R = 3.462 \times 10^8$ Pa, $Q = 7.86 \times 10^8$ Pa, $\beta = 3.06 \times 10^{-2}$ s, $S_L = 6.76 \times 10^6$ sN/m^4, $K = 0.303$, $\varepsilon_1 = 0.15$ and $\varepsilon_2 = 0.637$.

Figure 6(a) and (b) shows the deflection and moments varying with time. For long time, deflection and moments tend to their limits, i.e. $w = 0.00406$, $M_{11} = 0.0424$ and $M_p = 0$, respectively. It is worthwhile to point out that the moment M_p changes quickly from zero and shortly it decrease to

DOI: 10.1002/nag

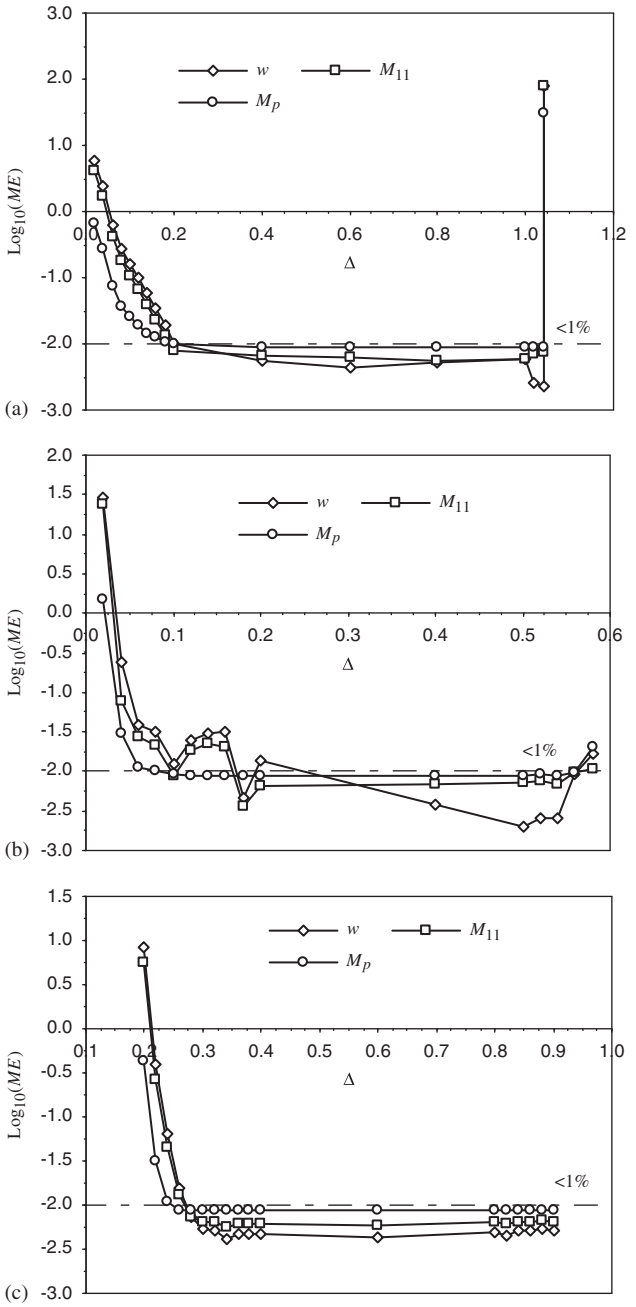

Figure 4. The relative mean error (*ME*) of the deflection and moments at the centre of plate: (a) normal distribution; (b) radial distribution; and (c) circular distribution. In this case, the total number of source point $N=76$, the material constants $K=0.5$, $\varepsilon_1=0.05$ and $\varepsilon_2=0.01$.

DOI: 10.1002/nag

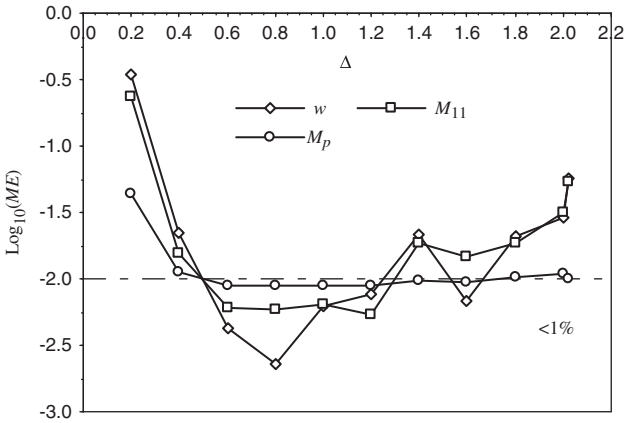

Figure 5. The relative mean error (*ME*) for the type I source point with source point $N=76$.

Table I. Information necessary for the computation of the plate response.

Lateral size, a(m)	1.0	Porosity, n_L	0.26
Lateral size, b(m)	1.0	Permeability, k	1.0×10^{-11}
Thickness, h (m)	0.05	Fluid viscosity, μ (Ns/m^2)	1.0×10^{-3}
Density, ρ_S (kg/m^3)	2260.0	Drained bulk modulus of elasticity K_0 (GPa)	4.6
Density of water, ρ_L (kg/m^3)	1000.0	Undrained bulk modulus of elasticity K_u (GPa)	8.3
Shear modulus, G (GPa)	4.2	Biot coefficient of effective stress, α	0.85
Poisson ratio, v	0.15		

zero again. In this example, the first type of source points distribution is selected, total number of source point $N=76$ and gap $\Delta=0.5$. The Fourier series solutions are plotted in these figures for comparison. Obviously, excellent agreements have been achieved.

The deflection and moments at the centre of plate with four edges built in are shown in Figure 7(a), (b) and (c) when parameters $K=0.5, 1, 2.5$ and $\varepsilon_1=\varepsilon_2=0.001$. The third type of source points distribution is utilized, the total number of source point $N=76$ and gap $\Delta=0.5$. The equivalent moment $M_p(t)$ is assumed to be zero on four edges. Furthermore, the selections of the number of sample point in the Laplace domain $L(>100)$, two free parameters η and T have slight influence on the numerical results. In addition, the densities ρ_S, ρ_L and the scalar parameter S_L are assumed to be constants in this numerical modelling. If these parameters are considered to be variables in the domain, an algorithm dealing with such non-linear problems must be developed. Obviously the MFS is not valid.

5.2. A circular poroelastic plate subjected to Heaviside load

A circular poroelastic plate of radius a carries a uniformly distributed Heaviside load of intensity $q(t)=q_0H(t)$ over the entire surface of the plate. The aim of this example is to demonstrate the application of MGS for the curved boundary. Poisson's ratio $v_S=0.3$ and the non-dimensional parameters are chosen as $K=0.5$, $\varepsilon_1=0.05$ and $\varepsilon_2=0.01$. Boundary values are

DOI: 10.1002/nag

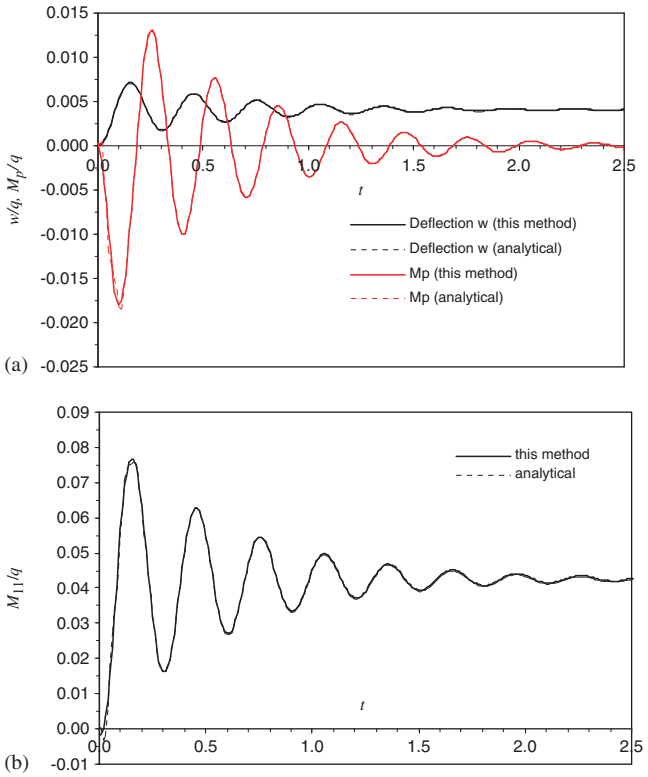

Figure 6. Comparisons with analytical solution: (a) deflection and equivalent moment and (b) moment. The parameters in Boit's model $K=0.303$, $\varepsilon_1=0.15$, $\varepsilon_2=0.637$.

given by $\tilde{w}_0=\tilde{M}_{n0}=\tilde{M}_{p0}=0$ for a simply supported plate. Deflection $w(t)$, moments $M_{11}(t)$ and $M_p(t)$ at the centre of plate for different parameter selection are shown in Figure 8(a), (b) and (c), respectively. At the beginning of time, all variables are zero as expected. However, the deflection $w(t)$ and moments $M_{11}(t)$ have limits of 0.00398 and 0.05156, respectively, which are the values of deflection and moment of circular plate under static uniform distributed load.

5.3. A square poroelastic plate under concentrated load

Finally, a simply supported square plate subjected to a concentrated shear force $PH(t)$ at the centre of the plate is investigated. The aim of this example is to check the fundamental solution of concentrated force. In the normalized procedure, we only need to change qa^2 to P in (18). Poisson's ratio v_S is 0.3. The first type of source point distribution is selected. Total number of source point $N=76$ and the gap between source point and boundary Δ are chosen as 0.6. As the moment $M_{11}(t)$ is of singularity at the point of concentrated force, we present deflection and moment near the centre of plate, i.e. $x_1=0.001$, $x_2=0$ in Figure 9(a) and (b), respectively, where parameters $\varepsilon_1=0.05$, $\varepsilon_2=0.01$ and $K=0.5$. Apparently for all examples, when normalized time $t>1.0$, there are only slight difference between dynamic solution and static solutions. However, at the beginning of time, the effect of fluid in the porous of plate is significant. The comparisons have

DOI: 10.1002/nag

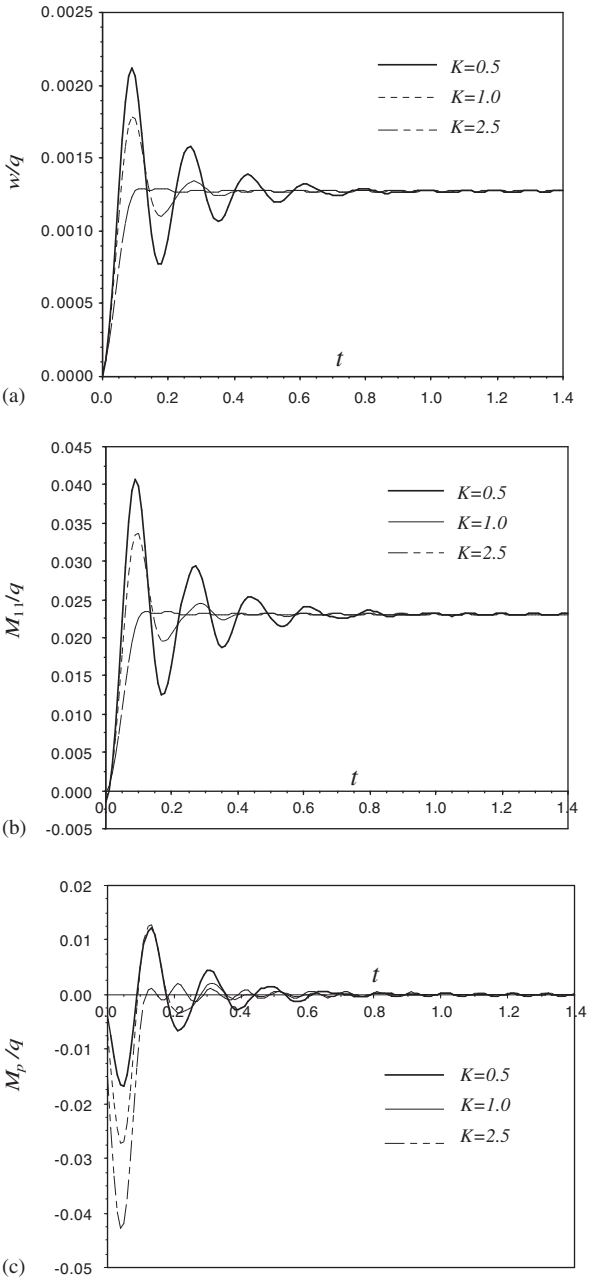

Figure 7. Results at the centre of plate with four edges clamped: (a) deflection; (b) moment; and (c) equivalent moment. The parameters in Boit's model $\varepsilon_1 = \varepsilon_2 = 0.001$.

DOI: 10.1002/nag

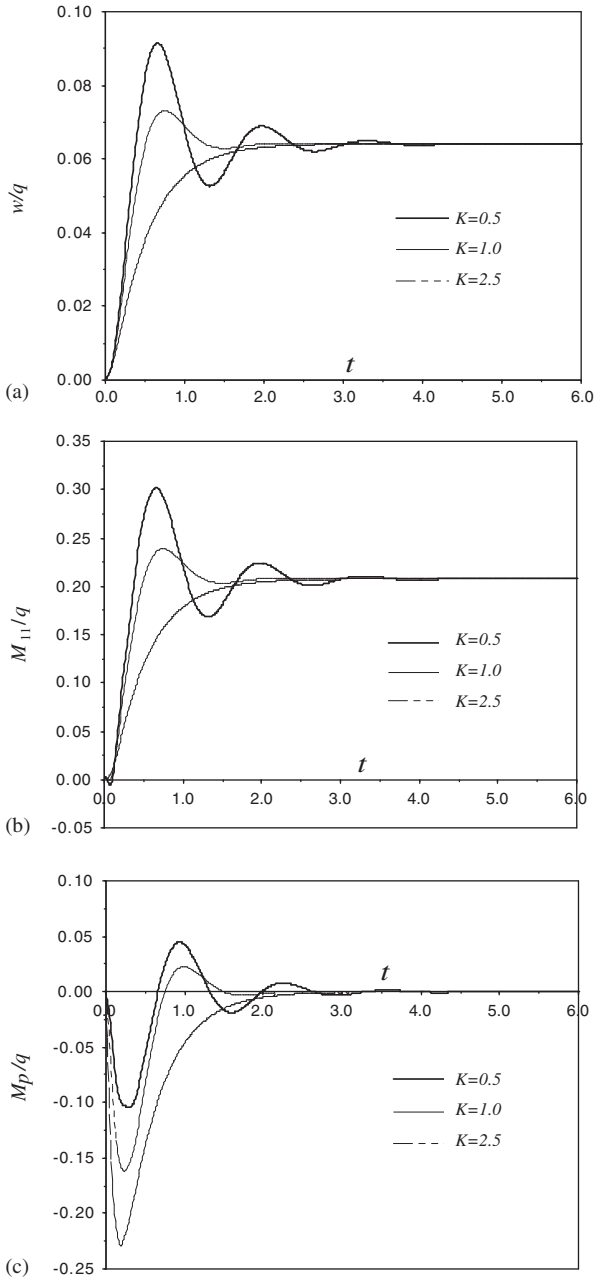

Figure 8. Results at the centre of circular plate with simply supported boundary: (a) deflection; (b) moment; and (c) equivalent moment. The parameters in Boit's model $\varepsilon_1 = 0.05$ and $\varepsilon_2 = 0.01$.

DOI: 10.1002/nag

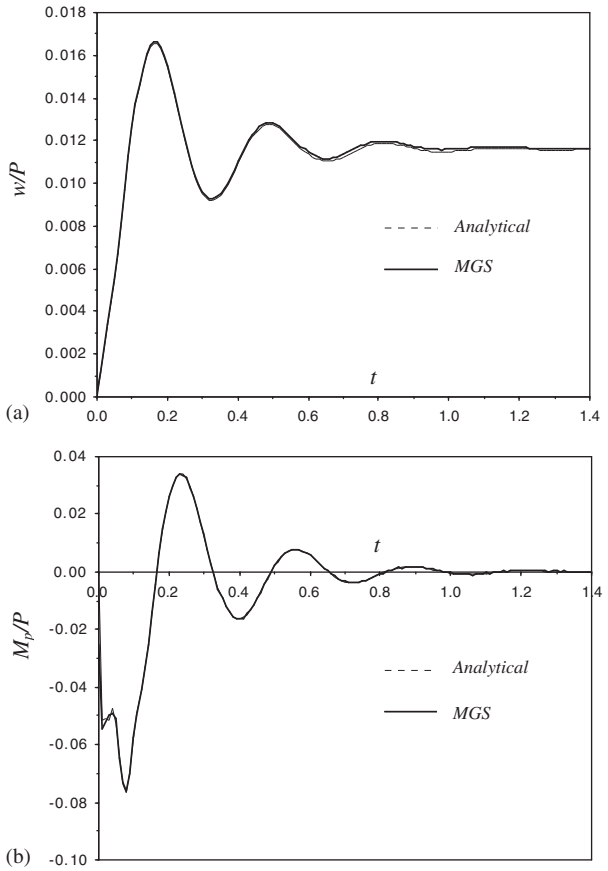

Figure 9. Results at the centre of square plate with simply supported boundary subjected to a concentrated force P: (a) deflection and (b) equivalent moment. In this case, the total number of source point $N=76$, the parameters in Boit's model are $K=0.5$, $\varepsilon_1=0.05$ and $\varepsilon_2=0.01$.

been made with the Fourier series method and show that the accuracy of the method proposed in this paper is very satisfied. Here two free parameters η and T are chosen to be 5 in this example.

6. CONCLUSIONS

In this paper, the fundamental solutions for the poroelastic thin plate were derived both in the Laplace transform domain and in the time domain. The method of fundamental solution (MFS) was demonstrated for dynamic problems. The accuracy and stability of the MFS was examined for dynamic case and the optimized gap between collocation and source point was studied. Excellent agreements with the analytical solution for a rectangular plate were achieved. Being one of the meshfree techniques, the MFS has most advantages of the meshfree method and demonstrates three major features in their computations: simplicity, accuracy and efficiency. Compared with the

DOI: 10.1002/nag

FEM and BEM, the MFS is more flexible and simple to program. However, the disadvantages of the MGS are also evident such as the optimized source point distribution needs to be investigated. Finally, the boundary integral formulations with the fundamental solution (concentrated force) can be derived directly.

APPENDIX A

Considering the boundary condition for a simply supported plate, the general solutions of deflection and moment can be written in the Fourier series as

$$\begin{aligned} w(t) &= \sum_{m=1}^{\infty}\sum_{n=1}^{\infty} w_{mn}(t)\sin m\pi x_1 \sin m\pi x_2 \\ M_p(t) &= \sum_{m=1}^{\infty}\sum_{n=1}^{\infty} M_{mn}(t)\sin m\pi x_1 \sin m\pi x_2 \end{aligned} \tag{A1}$$

Apparently these solutions satisfy all boundary conditions along four edges. Substituting (A1) into Equations (22a) and (22b) gives

$$w_{mn} + \frac{\psi_{mn}}{\varepsilon_2}\ddot{w}_{mn} + \frac{K(1-\varepsilon_1)^2+\varepsilon_2}{\varepsilon_2}\psi_{mn}^2\dot{w}_{mn} + \frac{\psi_{mn}^3}{\varepsilon_2}w_{mn} = \frac{\psi_{mn}}{\varepsilon_2}q_{mn} \tag{A2}$$

$$K(1-\varepsilon_1)\psi_{mn}\dot{w}_{mn} + \varepsilon_2\dot{M}_{mn} + \psi_{mn}M_{mn} = 0 \tag{A3}$$

where constants

$$\psi_{mn} = \pi^2(m^2+n^2), \quad q_{mn} = 4\int_0^1\int_0^1 q(x_1,x_2,t)\sin m\pi x_1 \sin m\pi x_2\,\mathrm{d}x_1\,\mathrm{d}x_2 \tag{A4}$$

For example, the analytical solution of deflection can be obtained, for a Heaviside load $q = H(t)$, by

$$w_{mn}(t) = \sum_{k=1}^{3} W_k \mathrm{e}^{\beta_k t} + \frac{q_{mn}}{\psi_{mn}^2} \tag{A5}$$

$$q_{mn} = \frac{4}{mn\pi^2}(1-\cos m\pi)(1-\cos n\pi) \tag{A6}$$

and for a concentrated force $q = H(t)\delta(x_1-0.5)\delta(x_2-0.5)$

$$q_{mn} = 4\sin\frac{m\pi}{2}\sin\frac{n\pi}{2} \tag{A7}$$

The equivalent moment in plate

$$M_{mn}(t) = C_{mn}\mathrm{e}^{-\psi_{mn}t/\varepsilon_2} - \sum_{k=1}^{3}\frac{K(1-\varepsilon_1)\psi_{mn}\beta_k}{\varepsilon_2\beta_k+\psi_{mn}}W_k\mathrm{e}^{\beta_k t} \tag{A8}$$

where non-dimensional parameters β_k are three roots of the following equation

$$\beta^3 + \frac{\psi_{mn}}{\varepsilon_2}\beta^2 + \frac{K(1-\varepsilon_1)^2+\varepsilon_2}{\varepsilon_2}\psi_{mn}^2\beta + \frac{\psi_{mn}^3}{\varepsilon_2} = 0 \tag{A9}$$

DOI: 10.1002/nag

Unknown coefficients W_k and C_{mn} can be determined by the following initial conditions

$$w_{mn}(0)=\dot{w}_{mn}(0)=M_{mn}=0, \quad \ddot{w}_{mn}(0)=q_{mn} \tag{A10}$$

Thus, we have

$$W_1+W_2+W_3=0 \tag{A11}$$

$$\beta_1 W_1+\beta_2 W_2+\beta_3 W_3=0 \tag{A12}$$

$$\beta_1^2 W_1+\beta_2^2 W_2+\beta_3^2 W_3=q_{mn} \tag{A13}$$

$$C_{mn}-\sum_{k=1}^{3}\frac{K(1-\varepsilon_1)\psi_{mn}\beta_k}{\varepsilon_2\beta_k+\psi_{mn}}W_k=0 \tag{A14}$$

Therefore,

$$W_1=\frac{q_{mn}}{(\beta_2-\beta_1)(\beta_3-\beta_1)}, \quad W_2=\frac{q_{mn}}{(\beta_1-\beta_2)(\beta_3-\beta_2)}, \quad W_3=\frac{q_{mn}}{(\beta_1-\beta_3)(\beta_2-\beta_3)} \tag{A15}$$

and

$$C_{mn}=\sum_{k=1}^{3}\frac{K(1-\varepsilon_1)\psi_{mn}\beta_k}{\varepsilon_2\beta_k+\psi_{mn}}W_k \tag{A16}$$

By using the constitutive relations for the thin plate bending in Equations (11) and (12), the components of moment and shear force can be determined in the time domain for a simply supported rectangular plate subjected to any kind of distributed dynamic load $q(x_1, x_2, t)$.

REFERENCES

1. Richardson J, Power H. A boundary element analysis of creeping flow past two porous bodies of arbitrary shape. *Engineering Analysis with Boundary Elements* 1996; **17**:193–204.
2. Biot MA. General theory of three-dimensional consolidation. *Journal of Applied Physics* 1941; **12**:155–164.
3. Biot MA. Theory of elasticity and consolidation for a porous anisotropic solid. *Journal of Applied Physics* 1955; **26**:182–185.
4. Corfdir A, Dormieux L. Mathematical model of flexure in a saturated geological layer: application to faulting. *Tectonophysics* 1998; **292**:267–278.
5. Hou JS, Holmes MH, Lai WM, Mow VC. Boundary conditions at the cartilage-synovial fluid interface for joint lubrication and theoretical verifications. *Journal of Biomechanical Engineering* 1989; **111**:78–87.
6. Kenyon DE. The theory of an incompressible solid–fluid mixture. *Archive for Rational Mechanics and Analysis* 1976; **62**:131–147.
7. Li LP, Cederbaum G, Schulgasser K. Theory of poroelastic plates with in-plane diffusion. *International Journal of Solids and Structures* 1997; **34**:4515–4530.
8. Mow VC, Holmes MH, Lai WM. Fluid transport and mechanical properties of particular cartilage: a review. *Journal of Biomechanics* 1984; **17**:377–394.
9. Wang ZH, Prevost JH, Coussy O. Bending of fluid-saturated linear poroelastic beans with compressible constituents. *International Journal for Numerical and Analytical Methods in Geomechanics* 2008; **33**:425–447.
10. Qiu T, Fox PG. Numerical analysis of 1-D compression wave propagation in saturated poroelastic media. *International Journal for Numerical and Analytical Methods in Geomechanics* 2007; **32**:161–187.
11. Barry SI, Parker KH, Aldis GK. Fluid-flow over a thin deformable porous layer. *Zeitschrift für angewandte Mathematik und Physik* 1991; **42**:633–648.
12. Wen PH, Hon YC, Wang W. Dynamic responses of shear flows over a deformable porous surface layer in a cylindrical tube. *Applied Mathematical Modelling* 2009; **33**:423–436.

DOI: 10.1002/nag

13. Pozrikidis C. *Boundary Integral and Singularity Method for Linearized Viscous Flow*. Cambridge University Press: Cambridge, 1992.
14. Wrobel LC. *The Boundary Element Method I*, *Applications in Thermo-fluids and Acoustics*. Wiley: New York, 2002.
15. Theodorakopoulos DD, Bescos DE. Flexural vibration of poroelastic plate. *Acta Mechanica* 1994; **103**:191–203.
16. Biot MA, Willis DG. The elastic coefficients of the theory of consolidation. *Journal of Applied Mechanics* 1957; **24**:594–601.
17. Leclaire P, Horoshenkov KV, Cummings A. Transvers vibrations of a thin rectangular porous plate saturated by a fluid. *Journal of Sound and Vibration* 2001; **247**(1):1–18.
18. Leclaire P, Horoshenkov KV, Swift MJ, Hothersall DC. The vibrational response of a clamped rectangular porous plate. *Journal of Sound and Vibration* 2001; **247**(1):19–31.
19. He L, Yang X. A dynamic bending model of incompressible saturated poroelastic plates with in-plane diffusion. *Chinese Journal of Solid Mechanics* 2008; **29**(2):121–128.
20. Cheng AHD, Cabral JJSP. Direct solution of ill-posed boundary value problems by radial basis function collocation method. *International Journal for Numerical Methods in Engineering* 2005; **64**:45–64.
21. Chen CS, Lee S, Huang CS. The method of particular solutions using Chebyshev polynomial based functions. *International Journal of Computational Methods* 2007; **4**(1):15–32.
22. Chen JT, Wu CS, Lee YT, Chen KH. On the equivalence of the Trefftz method and method of fundamental solutions for Laplace and biharmonic equations. *Computers and Mathematics with Applications* 2007; **53**:851–879.
23. Belytschko T, Lu YY, Gu L. Element-free Galerkin method. *International Journal for Numerical Methods in Engineering* 1994; **37**:229–256.
24. Atluri SN. *The Meshless Method* (*MLPG*) *for Domain and BIE Discretizations*. Tech Science Press: Forsyth, GA, U.S.A., 2004.
25. Boer R. Theoretical poroelasticity—a new approach. *Chaos*, *Solitons and Fractals* 2005; **25**:861–878.
26. Detournay E, Cheng AHD. Fundamentals of Poroelasticity, comprehensive rock engineering: principles, practice and projects. In *Analysis and Design Method*, Fairhurst C (ed.), vol. II. Pergamon Press: Oxford, 1993; 113–171.
27. Abramowitz M, Stegun IA. *Handbook of Mathematical Functions*. Dover Publications, ING.: New York, 1970.
28. Wen PH. Point intensity method of solving circular plate resting on elastic subgrade. *Engineering Mechanics* 1987; **4**(2):18–26.
29. Wen PH. Boundary collocation method for rectangular plate with free corners resting on the elastic foundation. *Shanghai Mechanics* 1989; **10**(1):71–77.
30. Wen PH. The fundamental solution of Mindlin plates resting on a elastic foundation in the Laplace domain and its applications. *International Journal of Solids and Structures* 2008; **45**:1032–1050.
31. Durbin F. Numerical inversion of Laplace transforms: an efficient improvement to Dubner and Abate's method. *Computer Journal* 1974; **17**(4):371–376.
32. Wen PH, Aliabadi MH, Rooke DP. The influence of elastic waves on dynamic stress intensity factors (three dimensional problem). *Archive of Applied Mechanics* 1996; **66**(6):385–394.

DOI: 10.1002/nag